

PAPER • OPEN ACCESS

Synthesis, characterization, and photocatalytic properties of nanocrystalline NZO thin films

To cite this article: D Aryanto *et al* 2018 *J. Phys.: Conf. Ser.* **985** 012025

View the [article online](#) for updates and enhancements.

Related content

- [Study on Photocatalytic Properties of TiO₂ Nanoparticle in various pH condition](#)
Nasikhudin, M Diantoro, A Kusumaatmaja et al.
- [Evaluation of the photocatalytic activity of iron oxide nanoparticles functionalized with titanium dioxide](#)
A Herrera, A Reyes and J Colina-Márquez
- [Synthesis, Characterization and Visible Light Photocatalytic of Fe₃O₄/CuO/TiO₂/Ag Nanocomposites](#)
Malleo Fauzian, Ardiansyah Taufik and Rosari Saleh

Synthesis, characterization, and photocatalytic properties of nanocrystalline NZO thin films

D Aryanto¹, E Hastuti², N Husniya², T Sudiro¹ and B W Nuryadin³

¹ Research Center for Physics, Indonesian Institute of Sciences, Tangerang Selatan, Indonesia

² Physics Department, Faculty of Science and Technology, UIN Maulana Malik Ibrahim, Malang, Indonesia

³ Physics Department, UIN Sunan Gunung Jati, Bandung, Indonesia

E-mail: didik_phys@yahoo.co.id

Abstract. Nanocrystalline Ni-doped ZnO (NZO) thin films were synthesized on glass substrate using sol-gel spin coating methods. The effect of annealing on the structural and optical properties of nanocrystalline thin film was studied using X-ray diffractometer (XRD), field emission scanning electron microscopy (FESEM), UV-VIS spectrophotometry, and photoluminescence (PL). The results showed that the annealing temperature strongly influenced the physical properties of nanocrystalline NZO thin films. The photocatalytic properties of nanocrystalline NZO thin films were evaluated using an aqueous solution of Rhodamine-B. The photocatalytic activity of nanocrystalline NZO thin films increased with the increase of annealing temperature. The results indicated that the structure, morphology, and band gap energy of nanocrystalline NZO thin films played an important role in photocatalytic activity.

1. Introduction

Photocatalysis based on metal oxide semiconductor has been considered as alternative materials for degrading recalcitrant organic compound in wastewaters [1]. Many metal oxides including CdS, TiO₂, Fe₂O₃, WO₃, and ZnO have been studied as fine powder for photocatalysis application [2 - 5]. The problem of using the powder photocatalysts is that they are difficult to separate, recovery, and recycle [1]. It generates potential health and environmental risks. These problems can be overcome by using thin films as photocatalysts. However, their photocatalytic activity is lower than the powder photocatalysts [1], caused by the reduction of the surface area. Accordingly, the surface morphology modification of thin films such as porosity, film homogeneity, and pore size distribution is indispensable to improve the photocatalytic activity [3, 6]. Besides, the doping of metallic and rare earth element can be used to modify films surface and enhance the photocatalytic performance [2, 7 - 10].

Among the metal oxide semiconductor, ZnO has several advantages such as relatively cheap, non-toxic and chemically stable [9]. ZnO is II-VI semiconductor compound with direct wide-band-gap of 3.37 eV and large exciton binding energy of 60 meV at room temperature [3, 11, 12]. It makes ZnO applicable as solar cell [13], laser [14], gas sensors [15], piezoelectric materials [16], and light emitting diodes (LEDs) [17]. In recent years, the function of ZnO as photocatalyst [2, 3, 7-9, 18-20]



and antibacterial agent [8, 11] has been investigated. This is owing to its excellent photocatalytic efficiency and good stability. Several studies show that the ZnO exhibits greater photocatalytic efficiency than TiO_2 to degrade organic pollutants [4]. However, due to its wide band gap, ZnO exhibits photocatalytic activity only under UV light [4, 8, 9]. It greatly inhibited their applications. Some studies reported that the optical response of ZnO into the visible light can be improved by doping it with transition metal elements such as Ag [9], Cu [2], Mn [21], Co [8], Mg [22], Cd [9] and Ni [19]. In particular, Ni is one of the most efficient doping elements to modify the band-gap of ZnO. The advantage of Ni metal over other metals like Ag, Mn, Pd, and Cd is due to its low cost. Furthermore, Ni ion has the same radius and valence-band with Zn ion, which results in large solubility in the ZnO matrix [23]. Some works on Ni-doped ZnO reported that the optical, electrical, and magnetic properties of ZnO were changed after Ni doping [24, 25]. However, little reports have been found to investigate the photocatalytic activity of Ni-doped ZnO thin films [12, 19]. In this work, Ni-doped ZnO (Ni = 3 at.%) thin films was fabricated using sol-gel methods. The effect of annealing on the structural, optical, and photocatalytic properties of ZnO thin films was discussed.

2. Experimental details

2.1. Synthesis of NZO thin films

Nanocrystalline NZO thin films were prepared on corning glass by sol-gel spin coating methods. First, corning glass substrate was cleaned sequentially with acetone, methanol and DI water in an ultrasonic bath and then dried. The NZO solution was prepared by mixing zinc acetate dihydrate ($\text{Zn}(\text{CH}_3\text{COO})_2 \cdot 2\text{H}_2\text{O}$), nickel acetate tetrahydrate ($\text{Ni}(\text{OCOCH}_3)_2 \cdot 4\text{H}_2\text{O}$), isopropanol and ethanolamine as precursor, dopant, solvent, and stabilizer, respectively. The molar ratio of isopropanol and zinc acetate dihydrate was maintained at 1.0 and the concentration of nickel was 3% from zinc. The resulted solution was stirred at 60 °C for 90 min and then aged for 24 hours at room temperature before usage. The NZO solution was then dropped on the corning glass substrate and rotated at 2500 rpm for 15 seconds using VTC-100 spin coater system. After deposition, the NZO films were preheated at 300 °C for 30 minutes to remove the solvent and then heated in air at 400, 500 and 600 °C for 1 hour.

2.2. Characterizations

The structure of nanocrystalline NZO thin films was studied with XRD-Smartlab Rigaku system. The surface morphology of the thin films was investigated by FESEM JIB-4610F system. The optical properties were determined using UV-Vis spectrophotometer UV-2600 Shimadzu and Photoluminescence Cary Eclipse Spectrophotometer Agilent Technology. All characterization was performed at room temperature.

2.3. Photocatalytic activity

The photocatalytic activity of NZO thin films was investigated by photodecolorization of the Rhodamine-B (RhB) solution under UV light. The experiment was carried out in home-made reactor at room temperature with Royalux T5 6 W lamps as UV source. The obtained films were placed inside 100 mL of a 10 ppm RhB solution with eight UV lamps. The photocatalytic degradation was evaluated by measuring the absorbance of RhB solution for every 30 min using visible spectrophotometer AMTAST AMV01. The degradation efficiency of RhB was calculated using equation in reference [8, 12].

3. Results and discussion

3.1. Structural properties

Figure 1 shows XRD patterns of nanocrystalline NZO thin films as a function of heat treatment temperature of 400, 500, and 600 °C. All samples show seven diffraction peaks corresponding to

(100), (002), (101), (102), (110), (103), and (112) planes of the ZnO (ICCD 01-078-3315). It indicates that all films have polycrystalline nature and hexagonal wurtzite structure [20]. The nickel metal and other oxide phases are not detected in the XRD pattern, suggesting that the Ni dopant has entered into the ZnO lattice. The atomic radii of Ni and Zn are almost equal which lead to no effect on the crystal orientation of nanocrystalline NZO films. Further observations show that there is no peak shifted from nanocrystalline NZO thin film after heat treatments, but slight changed in FWHM and intensity. The result reveals that the heat treatment has an effect on the crystal parameters, as shown in table 1.

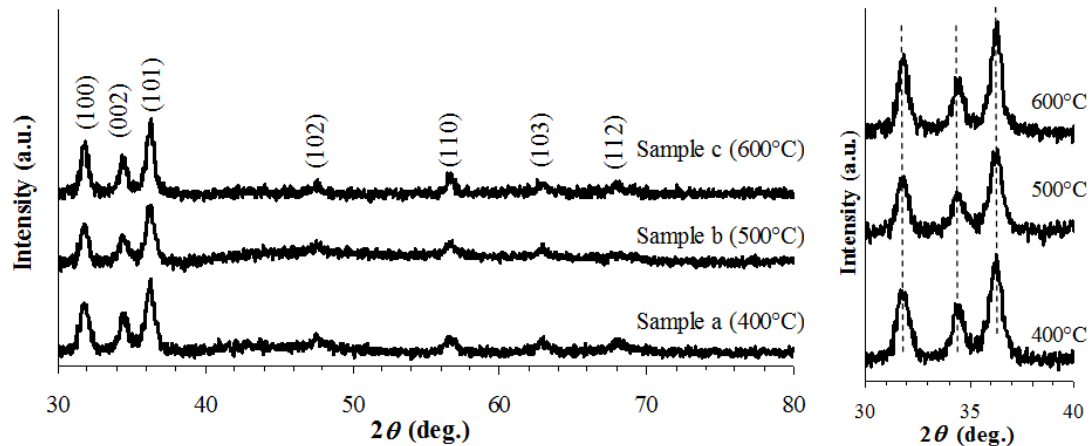


Figure 1. XRD patterns of NZO thin films.

The crystalline size (D), lattice strain (ε), residual stress (σ), and dislocation density (ρ) were estimated from equation 3 of reference [8], equation 4 of reference [26], equation 6 of reference [27], and equation 4 of reference [28], respectively. It can be seen in the table 1 that the crystalline size of film increases with increasing temperature. The mobility of the species on the surface occurs as the annealing temperature increases [26, 29, 30] which causes the diffusion at the grain boundaries. This phenomenon causes an agglomeration of small grains into larger grain and reduces the crystal defect. It was indicated by the decreasing in lattice strain and dislocation density as shown in the table 1. The calculation result of residual stress reveals that the Ni^{2+} on the ZnO lattice affects the compressive stress in the films [26]. The difference in the ionic radii between host material and the dopant influences the stresses arising. The crystal parameters of the film fabricated by sol-gel method are strongly influenced by heat treatment.

Table 1. Crystal parameter of nanocrystalline NZO thin films as effect of heating temperature.

Crystal parameters	Orientation								
	100			002			101		
	400 °C	500 °C	600 °C	400 °C	500 °C	600 °C	400 °C	500 °C	600 °C
FWHM	0.728	0.614	0.542	0.605	0.581	0.569	0.724	0.667	0.577
D (nm)	11.35	13.45	15.25	13.73	14.33	14.63	11.55	12.53	14.50
ε (%)	0.0112	0.0094	0.0083	0.0085	0.0082	0.0080	0.0096	0.0089	0.0077
σ (Gpa)	-2.608	-2.192	-1.931	-1.993	-1.906	-1.871	-2.245	-2.066	-1.788
ρ (line/nm ²)	0.0121	0.0086	0.0067	0.0563	0.0515	0.0496	0.0165	0.0140	0.0105

3.2. Morphological studies

The plane view of FESEM micrograph of nanocrystalline NZO thin films at different heating temperature is shown in figure 2. All films morphology consists of inhomogeneous grains which suggest that the nucleation of nanocrystalline NZO thin film on the substrate surface is non-uniform during crystal growth. Some pores can be seen in the morphology of nanocrystalline NZO thin film at heating temperature of 500 °C. The film becomes denser and the mean grain size of the films increases with increasing heating temperature. The increase of grain size was caused by coalescence of small grain [29]. This result corresponds to the XRD results as presented above.

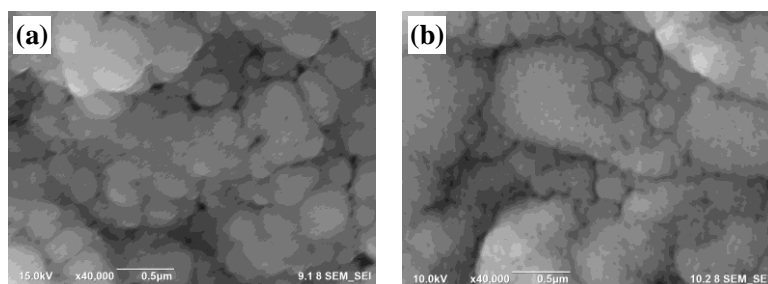


Figure 2. FESEM images of nanocrystalline NZO thin film heated at (a) 500 °C and (b) 600 °C.

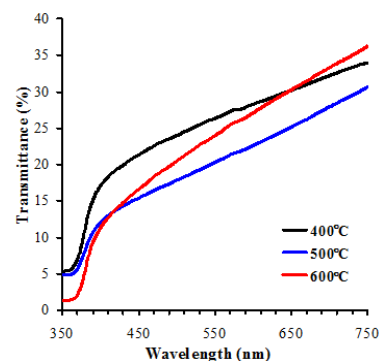


Figure 3. Transmission spectra of nanocrystalline NZO thin films heated at different temperatures.

3.3. Optical properties

Figure 3 shows the optical transmittance spectra of nanocrystalline ZnO thin films in the wavelength range of 350-750 nm. The transmittance spectra of all sample show a quite sharp absorption edge below 400 nm which is attributed to the fundamental absorption of zinc oxide [31, 32]. In figure 3, it can also be seen that all films exhibit low transmittance (less than 40%). The presence of Ni in the ZnO lattice promotes crystal defect as shown in XRD characterization, thus reducing the transmittance [33]. Besides that, inhomogeneous grains of NZO (as shown in figure 2) affect the optical scattering and contribute to the low transmittance [34].

The room temperature PL spectra of nanocrystalline NZO thin film as function of heating temperature are shown in figure 4. The PL spectra of all sample show several UV and visible emission, such as 361 nm (UV), 377 nm (UV), 421 nm (violet), 485 nm (blue), 495 nm (green), and 596 nm (orange). The UV emission originates from the recombination of free excitons and attributed to the near-band edge emission of ZnO [13, 27, 34]. The violet emission is due to the exciton transition from the localized level below the conduction band to the valance band [10]. Zhang et al. [35] reported that the blue emission originated from the electron transition from the shallow donor level of oxygen vacancies to the valance band, and electron transition from the shallow donor level of zinc interstitials to the valance band. The green emission may originate from the electron transition from the level of ionized oxygen vacancies to the valance band [18, 35]. The orange emission is attributed to oxygen interstitial in the ZnO system [30]. The PL intensity of nanocrystalline NZO thin film decreases with increasing heating temperature. It indicates that the defect concentration in the nanocrystalline NZO film decreases with the increasing heating temperature [13].

3.4. Photocatalytic activity

The photocatalytic activity of nanocrystalline NZO thin films on RhB solution under UV light irradiation is shown in figure 5a. No degradation of RhB solution in the absence of NZO films can be observed in figure 5a. The degradation also did not occur when UV lamp was not used (dark condition). This result indicates that the NZO thin films [36] and UV light [5] are essential for the

degradation of RhB. The significant enhancement in photocatalytic activity happened in nanocrystalline NZO thin film with heating temperature of 500 °C and 600 °C. Similar result has been reported by Lv et al. [10] where the photocatalytic activity of nanocrystalline ZnO thin films enhances with the increase of annealing temperature. The increase of structural, surface morphology, and optical properties are believed to have contributed in the acceleration of the photocatalytic activity.

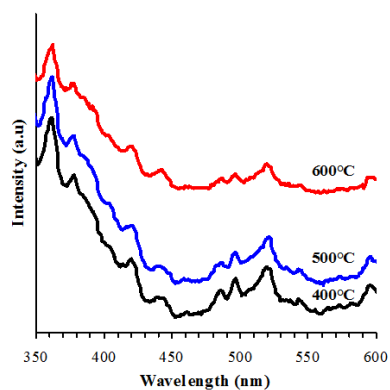


Figure 4. PL spectra of nanocrystalline NZO thin films heated at different temperatures.

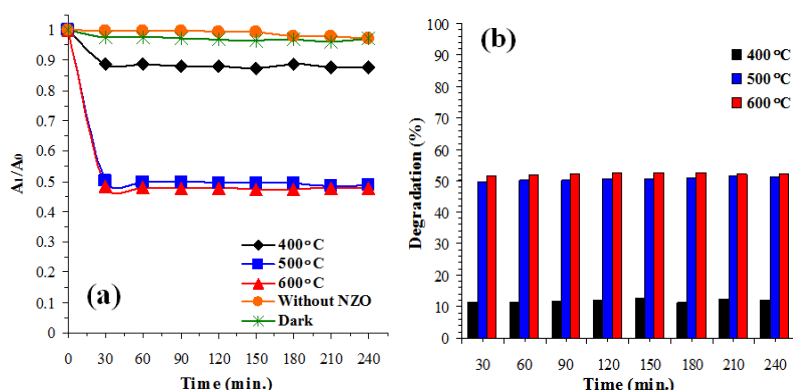


Figure 5. Photocatalytic (a) degradation and (b) degradation efficiency of RhB for nanocrystalline NZO thin films.

Figure 5b shows the photocatalytic degradation of RhB solution with nanocrystalline NZO thin films for an irradiation time of 240 min. The degradation efficiency of nanocrystalline NZO thin films increases to 12.15%, 51.23%, and 52.50% at elevated heat treatment temperature of 400 °C, 500 °C, and 600 °C, respectively. Increasing the crystallinity and mean grain size at heat treatment temperature of 500 °C and 600 °C affected the acceleration of photocatalytic activity. Besides, the Ni dopant in ZnO system generates the crystal defect such as oxygen vacancies, zinc interstitials, and oxygen interstitial. This result is shown in PL characterization (figure 4). The defect is considered to be the active sites of the ZnO photocatalyst because the redox reaction was probably occurred on the surface defects [10]. In general, the photocatalytic activity of thin films was influenced by the crystallinity and surface morphology of the film [3, 10].

4. Conclusion

Nanocrystalline NZO thin film has been synthesized by sol-gel spin coating method as a function of heat treatment temperature. All films have polycrystalline hexagonal wurtzite structure with inhomogeneous grains. The transmittance spectra of all film are below than 40% at the visible light. All films show several UV and visible emission in the PL spectra. The structural, surface morphology, and optical properties of nanocrystalline NZO thin film increased with increasing heating temperature. The photocatalytic activity of nanocrystalline NZO thin films enhances with increasing annealing temperature. It can probably be ascribed to the increase of crystallinity and the change in surface morphology. The presence of defect in the nanocrystalline NZO thin films also contributes to the photocatalytic activity.

Acknowledgments

The authors are very much thankful to Research Center for Physics, Indonesian Institute of Sciences for the financial support and thank also for Materials Research Laboratory- Physics Department, Faculty of Science and Technology, UIN Maulana Malik Ibrahim for the photocatalysis test facilities.

References

- [1] Ahumada-Lazo R, Torres-Martínez L M, Ruíz-Gómez M A, Vega-Becerra O E and Figueroa-Torres M Z 2014 *Appl. Surf. Sci.* **322** 35
- [2] Saidani T, Zaabat M, Aida M S and Boudine B 2015 *Superlattices Microstruct.* **88** 315
- [3] McLaren A, Valdes-Solis T, Li G and Tsang S C 2009 *J. Am. Chem. Soc.* **131** 12540
- [4] Hunge Y M, Mahadik M A, Moholkar A V and Bhosale C H, 2017 *Appl. Surf. Sci.* **420** 764
- [5] Wang C and Cao L 2011 *J. Rare Earth* **29** 727
- [6] Choi H, Stathatos E and Dionysiou D D 2007 *Desalination* **202** 199
- [7] Alam U, Khan A, Raza W, Khan A, Bahnemann D and Muneer M 2017 *Catal. Today* **284** 169
- [8] Poongodi G, Anandan P, Kumar R M and Jayavel R 2015 *Spectrochim. Acta A* **148** 237
- [9] Weng Y C and Hsiao K T 2015 *Int. J. Hydrog. Energy* **40** 3238
- [10] Lv J, Gong W, Huang K, Zhu J, Meng F, Song X and Sun Z 2011 *Superlattices Microstruct.* **50** 98
- [11] Podporska-Carroll J, Myles A, Quilty B, McCormack D E, Fagan R, Hinder S J, Dionysiou D D and Pillai S C 2017 *J. Hazardous Mater.* **324** 39
- [12] Kaneva N V, Dimitrov D T and Dushkin C D 2011 *Appl. Surf. Sci.* **257** 8113
- [13] Bedia A, Bedia F Z, Aillerie M, Maloufi N and Benyoucef B 2015 *Energy Procedia* **74** 529
- [14] Chu S, Olmedo M, Yang Z, Kong J and Liu J 2008 *Appl. Phys. Lett.* **93** 181106
- [15] Cittadini M, Sturaro M, Guglielmi M, Resmini A, Tredici I G, Anselmi-Tamburini U, Koshy P, Sorrell C C and Martucci A 2015 *Sens. Actuator B-Chem.* **213** 493
- [16] Fang T H and Kang S H 2010 *Curr. Nanosci.* **6** 505
- [17] Cole J J, Wang X, Knuesel R J and Jacobs H O 2008 *Nano Lett.* **8** 1477
- [18] Wu S, Chen Z, Wang T and Ji X 2017 *Appl. Surf. Sci.* **412** 69
- [19] Abdel-wahab M Sh, Jilani A, Yahia I S and Al-Ghamdi A A 2016 *Superlattices and Microstruct.* **94** 108
- [20] Salah N, Hameed A, Aslam M, Abdel-wahab M Sh, Babkair S S and Bahabri F S, 2016 *Chem. Eng. J.* **291** 115
- [21] Türkyılmaz Ş Ş, Güy N and Özacar M 2017 *J. Photochem. Photobiol. A* **341** 39
- [22] Abed C, Bouzidi C, Elhouichet H, Gelloz B and Ferid M 2015 *Appl. Surf. Sci.* **349** 855
- [23] Farag A A M, Cavaş M, Yakuphanoglu F and Amanullah F M 2011 *J. Alloys Compd.* **509** 7900
- [24] Rajeh S, Mhamdi A, Khirouni K, Amlouk M and Guermazi S 2015 *Opt. Laser Technol.* **69** 113
- [25] Yu M, Qiu H, Chen X, Li H and Gong W 2011 *Mater. Chem. Phys.* **126** 797
- [26] Chaitra U, Kekuda D and Rao K M 2017 *Ceram. Int.* **43** 7115
- [27] Fang D, Lin K, Xue T, Cui C, Chen X, Yao P and Li H 2014 *J. Alloys Compd.* **589** 346
- [28] Rao T P and Kumar M C S 2010 *J. Alloys Compd.* **506** 788
- [29] Belkhalifa H, Ayed H, Hafdallah A, Aida M S and Ighil R T 2016 *Optik* **127** 2336
- [30] Hasabeldaim E, Ntwaeaborwa O M, Kroon R E, Coetsee E and Swart H C 2017 *Opt. Mater.* **74** 139
- [31] Singh S, Srinivasa R S and Major S S 2007 *Thin Solid Films* **515** 8718
- [32] Hadri A, Taibi M, Ioghmarti M, Nassiri C, Tlemçani T S and Mzerd A 2016 *Thin Solid Films* **601** 7
- [33] Ying M, Wang S, Duan T, Liao B, Zhang X, Mei Z, Du X, Gerriu F M, Fox A M and Gehring G A 2016 *Mater. Lett.* **171** 121
- [34] Pati S 2017 *J. Alloys Compd.* **695** 3552
- [35] Zhang D H, Wang Q P and Xue Z Y 2003 *Appl. Surf. Sci.* **207** 20
- [36] Ali M B, Barka-Bouaifel F, Sieber B, Elhouichet H, Addad A, Boussekey L, Férid M and Boukherroub R 2016 *Superlattices and Microstruct.* **91** 225